Polyurethane Coatings Based on Chemically Unmodified Fractionated Lignin

Gianmarco Griffini,* Valeria Passoni, Raffaella Suriano, Marinella Levi, and Stefano Turri

Department of Chemistry, Materials and Chemical Engineering "Giulio Natta", Politecnico di Milano, Piazza Leonardo da Vinci 32, 20133 Milano, Italy

Received: January 29, 2015
Revised: March 20, 2015
Published: April 15, 2015

INTRODUCTION

In the quest for renewable and sustainable monomers and macromers for the production of high value-added polymeric materials, lignocellulosic feedstock potentially represents a promising and vast source of chemicals.[1] Lignocellulosic biomass is constituted by four main components, namely cellulose, hemicellulose, tannin and lignin, with lignin being by far the most abundant naturally occurring source of aromatics on Earth. At present, lignin is mostly produced as industrial residue in pulp and paper factories as well as in biorefineries.[2] The annual production of lignin from industrial waste streams is estimated in several million tons per year, with most of it being currently utilized as low-cost fuel for power and heat production. Only a little fraction is employed for commercial uses as filler, additive or dispersant in concrete, composites, binders or coatings.[3,4] However, these relatively low-value niche market applications only account for a minor fraction of the current worldwide lignin production, thus highlighting the urgent need of developing new strategies for the valorization of lignin as abundant macromolecular system for the production of high value-added, sustainable materials.

One strategy to exploit the enormous potential of lignin into value-added products is its use as building block for the preparation of lignin-based copolymers.[5,6] To this end, extensive efforts have been made to exploit lignin as the precursor of different classes of polymeric materials, including epoxies,[7−10] polyesters,[11−15] phenolics[16−18] and polyurethanes.[19−23] In particular, lignin-containing polyurethanes (PUs) have been widely investigated because of the high versatility of these materials that allows their potential use in different fields as elastomers, foams, coatings and adhesives. In this context, lignin can be considered as a renewable aromatic macropolyol that can potentially replace conventional fossil-derived polyols in PU synthesis, due to the high concentration of hydroxyl units (both phenolic and aliphatic) in its structure that can react with isocyanate (NCO) groups to achieve PU linkages.

The use of lignin as a macropolyol in PU synthesis commonly follows two general approaches. In the first approach, lignin undergoes chemical modifications (e.g., etherification, esterification, amination, oxypropylation) to allow hydroxyl functions to be more readily available for reaction with NCO groups.[5,6,24] Although this approach allows to improve the reactivity of −OH groups, chemical modification pretreatments of lignin may increase both the cost and the environmental impact of the resulting PUs, and

thus reduce their competitive advantage over conventional systems based on petroleum-derived polyols.[25] Accordingly, an alternative approach based on the direct use of lignin in coreaction with a suitable polyisocyanate without any preliminary chemical modification is usually preferable. To circumvent partially the relatively limited accessibility of −OH functions of lignin, other suitable polyols (e.g., poly(ethylene glycol), glycerol) are very often employed in the reactive mixture as comonomers and/or reactive cosolvents so that a reduction of the chemical steps to obtain the final PU material can be achieved, together with a prospective reduction of polymer processing costs.[26] In addition, these added polyols may also act as soft segments in the architecture of the PU system, imparting higher flexibility to the resulting material. Following this latter strategy, the production of several lignin-based PU materials has been demonstrated in the last decades, with a great deal of work being primarily focused on the development of rigid and flexible lignin-based PU foams and elastomers.[27−31] Very recently, thermoplastic lignin-based PUs with high lignin content (65−75 wt %) were also developed by reacting high-molecular-weight lignin with a rubbery diisocyanate, yielding a two-phase morphological arrangement that was found to be responsible for the thermoplastic rubbery behavior of the resulting PU material.[32,33] Although this represents an interesting approach to achieve polymeric recyclable materials based on lignin that can potentially lead to the development of partially carbon-neutral thermoplastics, the use of formaldehyde (a known carcinogenic substance) in the chemical pretreatment of lignin to increase its molecular weight inevitably limits the applicability of this strategy on a large scale.

As opposed to the case of PU foams and thermoplastics, few examples of lignin-based thermoset PUs have been proposed so far for use as coating materials and adhesives,[21,34−36] despite their great potential in the field of advanced sustainable manufacturing. Furthermore, no examples of high-lignin-content thermoset PUs based on the direct reaction of chemically unmodified lignin with a polyisocyanate without the use of additional polyols as comonomers have been presented in the literature to date. Finally, conventional petroleum-derived organic solvent media are commonly used during PU preparation and processing. However, the use of biobased solvents[37] should be preferable in view of a reduction of the environmental impact of chemical processes on a global scale and toward the development of more sustainable PU systems, notwithstanding their current higher costs compared with conventional systems.

Herein, novel high-lignin-content thermoset PU coatings are presented obtained by cross-linking commercial softwood kraft lignin with an aromatic polyisocyanate based on toluene diisocyanate (TDI) at different NCO/OH ratios. To improve the processability of lignin, solvent fractionation was performed on the commercial lignin sample prior to reaction with the TDI-based polyisocyanate by means of 2-methyl tetrahydrofuran (MeTHF), a biobased solvent obtainable from lignocellulosic biomass. The same solvent was then used for the preparation of the PU coatings. The effect of the NCO/OH ratio on the extent of the cross-linking reaction was examined and correlated with the theoretical and actual availability of hydroxyl groups in lignin as found from ^{13}C NMR spectroscopy. The chemical, physical, thermal, morphological, surface and wettability properties of the obtained PU coatings were thoroughly characterized by means of different techniques. In addition, the mechanical properties (elastic modulus) of the coatings were investigated through force−distance curve measurements by atomic force microscopy (AFM). Finally, the adhesion strength of these coatings on different substrates (glass, metal, wood) was evaluated by means of the pull-off method[38] and the potential use of these materials as adhesives was discussed.

The results of this study clearly demonstrate that the direct reaction of chemically unmodified lignin with polyisocyanates represents a viable and straightforward strategy for the development of advanced high lignin content PU systems and highlight the potential of lignin-based thermoset PUs as bioderived materials for application in the field of high-performance coatings and adhesives.

EXPERIMENTAL SECTION

Materials. All materials employed in this study are commercially available. Softwood kraft lignin (Indulin AT) was supplied by MeadWestvaco. Desmodur L75, an aromatic polyisocyanate based on a toluene diisocyanate (TDI)−trimethylolpropane adduct (TMP) (NCO content 13.3 wt %), was supplied by Bayer Material Science (see the Supporting Information for molecular structure). The bioderived solvent used for lignin fractionation and PU preparation was 2-methyltetrahydrofuran (MeTHF), supplied by Sigma-Aldrich.

Lignin Fractionation and Extraction. Lignin samples were fractionated by extraction with boiling MeTHF in order to obtain a lignin fraction suitable for further analysis and for material preparation. In a typical extraction process, 4 g of lignin was added to 150 mL of MeTHF in a round-bottomed flask equipped with a Soxhlet extractor. The temperature was raised to 80 °C and the extraction process was allowed to proceed for 8 h under vigorous magnetic stirring. After solvent extraction, the MeTHF-soluble lignin fraction was recovered as a brown solid by rotary evaporation, or directly used for PU preparation. The extraction yield was 50 ± 5%.

Polyurethane Synthesis and Film Preparation. Polyurethane (PU) materials were prepared by reaction of the MeTHF-soluble lignin fraction (from here on referred to as S-lignin) with Desmodur L75 (from here on referred to as TDI) at varying proportions. The desired amounts of S-lignin (dried overnight in a vacuum oven prior to use) and TDI were dissolved at room temperature in MeTHF (20 wt % concentration) under magnetic stirring (30 min). Subsequently, the S-lignin/TDI mixture was spin-cast onto glass substrates in air (1200 rpm, 40 s) by means of a WS-400B-NPP spin-processor (Laurell Technologies Corp.) and allowed to cross-link in a ventilated oven at 120 °C for 1 h. The extent of the reaction between OH groups in S-lignin and NCO groups in TDI was monitored by means of Fourier-transform infrared (FTIR) spectroscopy (disappearance of the N═C═O stretching signal at 2270 cm^{-1}). In addition, the completion of the cross-linking reaction on cast PU films was evaluated in terms of resistance to solvent washing (immersion in THF for 24 h) and solvent rubbing (MEK double rub test[39]). Because the ultimate aim of this work was to develop a high-lignin-content PU system, attempts were made to employ the lowest amount of TDI during the preparation of the final PU material. Accordingly, increasing S-lignin/TDI weight ratios were investigated, namely 70/30, 75/25, 80/20, 85/25 and 90/10, corresponding to theoretical NCO/OH molar ratios of 0.16, 0.12, 0.09, 0.07 and 0.04, respectively. Such theoretical NCO/OH values were calculated on the basis of the total hydroxyl content (both aliphatic and phenolic) determined from ^{13}C NMR analysis on acetylated S-lignin samples (see the following discussion).

Materials Characterization. *Gel Permeation Chromatography (GPC).* The molecular weight of lignin samples was estimated by means of gel permeation chromatography (GPC) using a Waters 510 high-performance liquid chromatography (HPLC) system equipped with a Waters 486 tunable absorbance detector set at λ = 300 nm, using THF as eluent. The sample (200 μL of lignin in THF, 2 mg/mL) was injected into a system of columns connected in series (Ultrastyragel HR, Waters) and the analysis was performed at 30 °C and at a flow rate of 0.5 mL/min. The GPC system was calibrated

against polystyrene standards in the 102−104 g/mol molecular weight range. As opposed to S-lignin, the parent unfractionated lignin Indulin AT was acetylated in order to make it soluble in the eluent following a procedure reported in the literature.[24]

^{13}C NMR. The amount of hydroxyl groups (aliphatic and aromatic) in S-lignin was evaluated by means of quantitative ^{13}C NMR spectroscopy on acetylated samples. ^{13}C NMR analysis was performed on a Bruker Avance 500 spectrometer in DMSO-d_6. The chemical shifts of the peaks in the spectra were referenced to the chemical shift of DMSO-d_6 (δ = 39.5 ppm) and the spectra were obtained with a 200 ppm spectral width, 32 000 points of acquisition, a relaxation delay of 12 s and a 4 Hz line broadening.

Fourier-Transform Infrared Spectroscopy (FTIR). FTIR spectra (64 accumulated scans at a resolution of 2 cm^{-1} in the 4000−700 cm^{-1} wavenumber range) were recorded in transmission mode at room temperature in air by means of a Nicolet 760-FTIR spectrophotometer on PU films spin-cast (1200 rpm, 40 s) from 20 wt % solutions in MeTHF onto KBr disks at varying lignin/TDI ratios. A constant thickness of 1.6 μm was obtained on all deposited PU films as measured by optical profiler (Microfocus, UBM) irrespective of the lignin/TDI ratio, thus allowing comparisons between the recorded FTIR spectra.

Differential Scanning Calorimetry (DSC). Differential scanning calorimetry (DSC) was carried out on solid state samples using a Mettler-Toledo DSC/823e instrument at a scan rate of 20 °C/min under nitrogen flux.

Thermogravimetric Analysis (TGA). Thermogravimetric analysis (TGA) was performed on solid state samples by means of a Q500 TGA system (TA Instruments) from ambient temperature to 800 °C at a scan rate of 10 °C/min both in air and nitrogen.

Optical Contact Angle (OCA). Static optical contact angle (OCA) measurements on the PU films were performed at room temperature using an OCA 20 (Data Physics) equipped with a CCD photocamera and with a 500 μL Hamilton syringe to dispense liquid droplets. A minimum of 25 measurements were taken in different regions on the surface of each PU film and results were averaged. Water (H_2O) and diiodomethane (CH_2Cl_2) were used as probe liquids.

Atomic Force Microscopy (AFM). Atomic force microscopy (AFM) imaging measurements were performed on the PU films by means of an NSCRIPTOR system driven by SPMCockpit software (NanoInk., Skokie, IL) in tapping mode with a scan rate of 0.3 and 0.2 Hz using commercially available silicon ACT-SS probes purchased from AppNano (Santa Clara, CA). Nanoindentation measurements were performed with the NSCRIPTOR instrument in ambient conditions (temperature in the 20−23 °C range and relative humidity between 25% and 40%) using commercially available silicon ACT probes purchased from AppNano (Santa Clara, CA) with a nominal spring constant of 40 N/m. The actual value of spring constants was calculated using the Sader method.[40] The elastic modulus of the samples under investigation was obtained from force−distance curve measurements based on the Sneddon model.[41] According to Sneddon, the relation between the deflection d and the indentation δ can be written as follows

$$d = \frac{2}{\pi}\frac{E_s}{(1-\nu_s^2)}\frac{\tan\vartheta}{k}\cdot\delta^2 \quad (1)$$

where E_s is the elastic modulus of the coating (assuming an infinitely higher modulus of the probe compared to the sample), ν_s its Poisson ratio, which was assumed to be equal to 0.35 for lignin-based PU film,[42] ϑ the half-opening angle of the silicon tip (~24° in our case, according to SEM images obtained after indentations)[43] and k the spring constant of probe cantilever. The value of Young's modulus was calculated by interpolating the curves with the Sneddon model in the region of reversible elastic deformations according to the method developed in a previous paper.[43]

Adhesion Tests. The adhesion of the PU films on different substrates (glass, wood, aluminum, stainless steel) was evaluated with a PosiTest AT-M Manual adhesion pull-off tester (DeFelsko) by measuring the pulling force needed to detach a 20 mm-diameter aluminum dolly adhered to the PU film by means of epoxy adhesive (Araldite 2011, curing cycle: 50 °C, 24 h).

RESULTS AND DISCUSSION

Available lignin grades possess a very heterogeneous structure and are usually characterized by a broad distribution of molecular weights and functional groups, which makes them relatively difficult to process, especially in view of their use in the preparation of high value-added polymeric materials. To partially overcome this limitation, solvent extraction is a commonly used technique to obtain relatively more homogeneous and more easily processable fractions of lignin by treating the parent material with common fossil-derived organic solvents and subsequently recovering the relative soluble and/or insoluble fractions for further use. In this way, the extracted lignin fraction can be more easily incorporated into bioderived polymeric materials by means of consolidated solution-based processing techniques. Along these lines, in this work fractionation of a commercial softwood kraft lignin was performed. However, as opposed to most of the recent literature studies involving lignin solvent extraction, a bioderived solvent system (MeTHF) was employed herein for the fractionation of the as-received lignin sample, in line with the global trend of resorting to more sustainable processing conditions and chemicals to limit the environmental impact of chemical processes on a broader perspective. As a result, a MeTHF-soluble lignin fraction could be obtained, thus allowing the use of such biobased solvent for the successive processing steps involved in the preparation of the PU materials under study.

Gel Permeation Chromatography (GPC). To evaluate the effect of solvent fractionation on the molecular weight distribution of lignin materials, the molecular weight of the as-received lignin (A-lignin) as well as of the MeTHF-soluble lignin fraction (S-lignin) was determined by GPC analysis. The as-received parent lignin exhibited poor solubility in the GPC eluent (THF); therefore, acetylation of this lignin sample was required. To allow for consistent comparisons, S-lignin was also subjected to the acetylation process prior to GPC analysis, despite its complete solubility in THF. Figure 1 reports the GPC chromatograms of the acetylated A-lignin and S-lignin systems investigated. The as-received A-lignin shows a broad

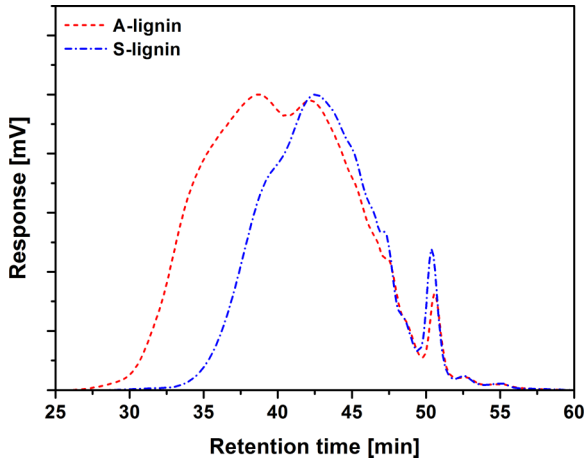

Figure 1. GPC chromatograms of as-received lignin (A-lignin) and MeTHF-soluble lignin fraction (S-lignin). Both samples were analyzed after acetylation.

molecular weight distribution with a partially bimodal profile. As opposed to this, the S-lignin fraction exhibits a narrower molecular weight distribution shifted toward higher retention times (t_R). Common to both samples is the presence of two distinct regions, namely a high-molecular weight (HMW) peak region (retention times before t_R = 49 min) and a low-molecular-weight (LMW) peak region (higher t_R), in accordance with previous works.[44] Quantification of the real abundance of the various species is difficult by GPC with UV detection, because they may show different UV sensitivity (i.e., extinction coefficient). However, in both acetylated samples, the LMW peak is found to account for about 6% of the HMW peak (in the case of A-lignin, the HMW area employed in the calculation is identified as the area included between t_R = 40 min and t_R = 50 min).

As presented in Table 1, the parent A-lignin shows M_n = 1980 g/mol and a polydispersity index (PDI) of 2.4, whereas

Table 1. Molecular Weights (M_n and M_w) and Polydispersity Index (PDI) of as-Received Acetylated Lignin (A-lignin) and MeTHF-Soluble Acetylated Lignin Fraction (S-lignin)

	M_n [g/mol]	M_w [g/mol]	PDI
A-lignin	1980	4680	2.4
S-lignin	1310	2320	1.8

lower molecular weights and smaller PDI values are found for S-lignin (M_n = 1310 g/mol with PDI = 1.8). These results are in agreement with literature reports on similar systems.[45] These results demonstrate that biosolvent fractionation represents a convenient "green" technique to isolate LMW lignin with a relatively narrow molecular weight distribution, and obtain a lignin fraction that is suitable for the preparation of high value-added polymeric materials via conventional solution-based processing approaches.

^{13}C NMR. To evaluate the reactivity of the lignin samples toward NCO groups, determination of their hydroxyl content was performed by means of quantitative ^{13}C NMR spectroscopy on both as-received A-lignin and fractionated S-lignin after acetylation. For the determination of the hydroxyl (aliphatic and phenolic) content, the number of carbon atoms associated with OH groups (aliphatic or aromatic) per aryl unit was first determined. Subsequently, the actual molar concentration (mmol/g) of OH groups in each lignin sample was calculated on the basis of the molecular weight of the PPU, the latter assumed to be 184 g/mol for kraft lignin.[24] In the ^{13}C NMR spectra, the following integration intervals were considered: primary aliphatic hydroxyls δ = 170.4−169.4 ppm, secondary aliphatic hydroxyls δ = 169.4−168.5 ppm, phenolic hydroxyls δ = 168.5−165.8 ppm, aromatic carbons δ = 160−100 ppm. The integration of the peaks in the region of the aromatic carbon atoms (δ = 160−100 ppm) was set as the reference for all ^{13}C NMR signals and was taken equal to 6, based on the assumption that this region includes six aromatic carbon atoms and that each PPU contains one aryl unit (six aromatic carbons). As shown in Table 2, a decrease of the aliphatic (primary and secondary) hydroxyl group content is observed upon MeTHF fractionation, leading to a total aliphatic hydroxyl groups content of 3.86 mmol/g.

As opposed to this, an increase in the concentration of phenolic hydroxyls OH(Φ) after solvent treatment is observed from 3.75 mmol/g (A-lignin) to 4.67 mmol/g (S-lignin). Overall, a slight decrease of OH functionalities is found in the

Table 2. Hydroxyl Group Content (mmol/g) of as-Received and MeTHF-Soluble (S-) Lignins Obtained from ^{13}C-NMR Spectra (Aliphatic Primary OH(I), Aliphatic Secondary OH(II) and Phenolic OH(Φ) Hydroxyl Groups)

	OH(I)	OH(II)	OH(Φ)	OH(total)
A-lignin	3.21	2.01	3.75	8.97
S-lignin	2.39	1.47	4.67	8.53

solvent-extracted lignin fraction (8.53 mmol/g) as compared to the parent lignin (8.97 mmol/g). These values are in close agreement with recent literature reports on similar softwood kraft lignins.[22,24]

Fourier-Transform Infrared Spectroscopy (FTIR). For the preparation of lignin-based PU films, S-lignin was reacted with the TDI cross-linker at varying weight ratios (70/30, 75/25, 80/20, 85/15, 90/10) and the intensity of the NCO stretching signal (2270 cm^{-1}) in the FTIR spectra of the resulting materials was used as a probe of the reaction between OH groups in lignin and NCO groups in the TDI. Cross-linking was conducted for 60 min at 120 °C. As inferred from the FTIR spectra of the PU materials presented in Figure 2,

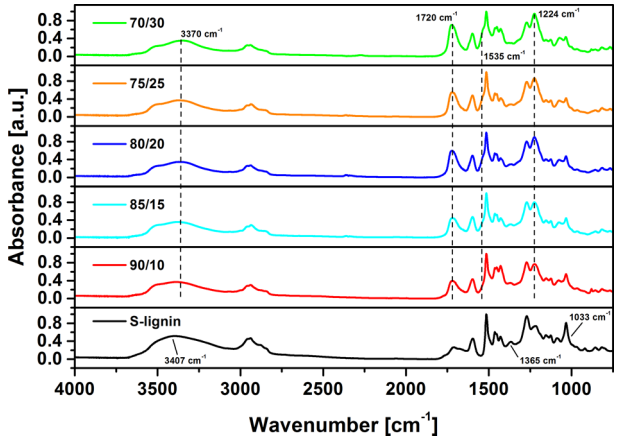

Figure 2. FTIR spectra of MeTHF-soluble lignin fraction (S-lignin) and of lignin-based PU materials at varying S-lignin/TDI weight ratios (70/30, 75/25, 80/20, 85/15, 90/10).

complete disappearance of the NCO stretching signal could be registered only for a S-lignin/TDI ratio of 75/15 or higher, whereas a residual NCO stretching signal could still be observed for lower S-lignin concentrations (70/30). This evidence indicates that only a minor portion of all OH groups present in the S-lignin polymer (8.53 mmol/g as obtained from ^{13}C NMR) is readily available for reaction with the NCO groups of the TDI cross-linker, likely due to steric hindrance of the hydroxyl functionalities resulting from the highly branched three-dimensional structure of lignin.[23,46] To estimate the amount (mmol) of hydroxyl groups actually available for the reaction with the isocyanate groups in the TDI cross-linker to form urethane bonds, stoichiometric calculations were performed based on the following considerations. The 75/25 PU formulation identifies the maximum weight content of TDI in the PU material that allows full reaction of NCO groups with OH groups in S-lignin and hence the maximum number of moles of hydroxyl groups actually available for reaction with the isocyanate moieties in the TDI. Indeed, complete disappearance of the NCO stretching signal in the FTIR spectrum is observed at a 75/25 S-lignin/TDI ratio, while higher TDI

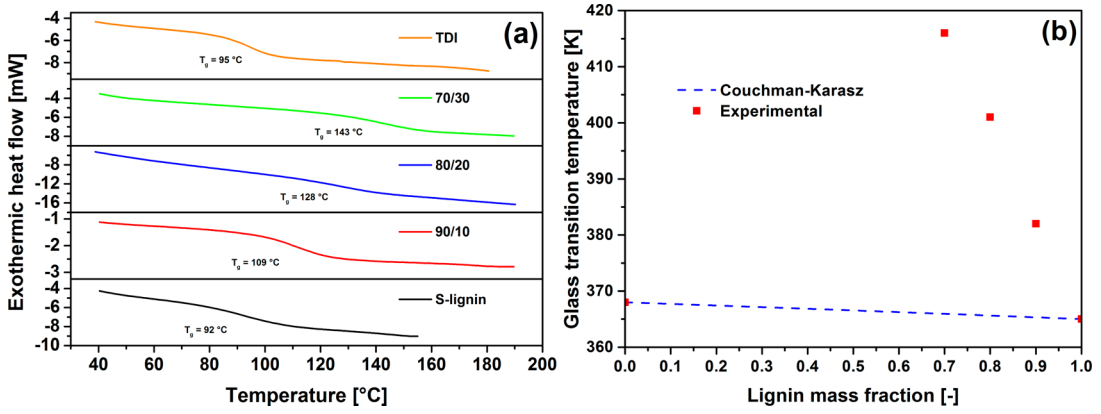

Figure 3. (a) DSC scans and glass transition temperature values (T_g) of MeTHF-soluble lignin fraction (S-lignin), TDI and of lignin-based PU materials at varying S-lignin/TDI weight ratios (70/30, 80/20, 90/10); (b) dependence of T_g on lignin mass fraction as obtained from the Couchman-Karasz equation (k_{CK} = 1.08) and from experimental DSC measurements.

contents yield the presence of residual FTIR NCO stretching signal. In accordance with these observations, assuming for the 75/25 PU material a stoichiometric reaction between OH groups in S-lignin and NCO groups in the TDI (that is, the molar ratio of isocyanates to hydroxyls NCO/OH is 1), a maximum number of reactive OH groups of 1.05 mmol/g was found to be readily available for reaction with isocyanates in the TDI. As a result, actual NCO/OH molar ratios of 1.3, 1, 0.7, 0.5 and 0.3 are obtained for S-lignin/TDI weight ratios of 70/30, 75/25, 80/20, 85/15 and 90/10, respectively. These results clearly indicate that only a minor portion of the OH groups present in lignin can actually be directly exploited for reaction with NCO groups to form urethane bonds.

In addition, to monitor the reaction between OH groups in S-lignin and NCO groups in TDI, FTIR spectroscopy was also used to investigate the chemical structure of the lignin-based PU films. As shown in Figure 2, a progressive decrease of the OH stretching signal present in S-lignin (3407 cm^{-1}) is observed upon reaction with increasing amounts of TDI, ultimately resulting in the formation of a shoulder at 3488 cm^{-1}. Concurrently, the appearance of a peak at lower frequencies (3370 cm^{-1} for 75/25 PU material) is also observed ascribed to N—H stretching vibrations and clearly indicating the formation of the N−H bond in urethanes. While a weak signal (shoulder) at 1710 cm^{-1} is observed in unreacted S-lignin ascribable to C═O stretching in conjugated carbonyl moieties present in the parent material, a sharp peak is found in the FTIR spectrum of all PU materials at 1720 cm^{-1}, resulting from C═O stretching vibrations of carbonyl groups in the urethane moiety. In addition, a broadening toward higher frequencies of the signal related to the aromatic skeletal vibrations in S-lignin (1515 cm^{-1}) is observed in the PU materials at increasing TDI content with the formation of a shoulder at 1535 cm^{-1}, likely originating from the contribution of C═O stretching vibrations in the forming urethane cross-link. The peak observed in S-lignin at 1365 cm^{-1} ascribable to phenolic OH stretching vibrations is found to progressively decrease in intensity in the PU material at increasing TDI concentration, likely due to reaction with NCO groups in TDI. Similar trends are observed for the sharp FTIR signal at 1033 cm^{-1} in unreacted S-lignin. As opposed to this, a peak at 1224 cm^{-1} is observed in the FTIR spectrum of PU materials whose intensity is found to increase with increasing TDI content. Such a signal may be assigned to C—N stretching vibrations in the urethane moiety, thus further confirming the successful formation of urethane cross-links in the lignin-based PU materials. Finally, a sharp decrease of the signal centered at 1033 cm^{-1} in S-lignin and ascribable to C—O deformations in primary alcohols is observed at increasing TDI content in the PU materials. These results suggest that the S-lignin material was covalently bonded via urethane cross-links with the TDI to yield a cross-linked lignin-based PU material.

Evidence of the reaction between S-lignin and TDI was further obtained by testing the solvent resistance (MEK double rub test[39]) of cast PU films at varying S-lignin/TDI weight ratios. Only PU films with an S-lignin/TDI weight ratio of 80/20 or lower (i.e., increasing concentration of TDI) were found to withstand more than 100 MEK double rubs, suggesting the presence of a chemically cross-linked structure and thus chemical interaction between S-lignin and TDI. On the contrary, for higher S-lignin/TDI weight ratios, partial or complete dissolution of the film was observed (60 and 25 double MEK rubs for 85/15 and 90/10 PU materials, respectively). To evaluate further the extent of cross-linking, additional tests were carried out on the 80/20 cross-linked systems by immersion of the PU films in THF for 24 h and by gravimetric assessment of the extracted sol fraction. Approximately 30% of nonreacted lignin was found to be extracted after immersion in THF for 24 h, with no further extraction observed for longer immersion times. These results further confirm that only a limited portion of OH groups in lignin is readily available for reaction with NCO groups in the TDI prepolymer, as also inferred from FTIR analysis of the extracted sol fraction where a significantly lower amount of OH groups in the extracted material (lower relative intensity of the OH stretching signal in the FTIR spectrum at 3407 cm^{-1}) is found compared to pristine lignin (see the Supporting Information). However, the presence of such nonreacted lignin material does not hamper the cross-linking reaction and the formation of a three-dimensional polymer network, as after extraction of the sol fraction, no further material loss was observed even after 72 h of immersion in THF.

Differential Scanning Calorimetry (DSC). The thermal transitions in S-lignin and in the lignin-based PU materials at varying S-lignin/TDI ratios were investigated by means of DSC analysis. As shown in Figure 3, the MeTHF-soluble lignin shows a glass transition temperature T_g of 92 °C, whereas the model urethane phase obtained by end-capping the TDI with

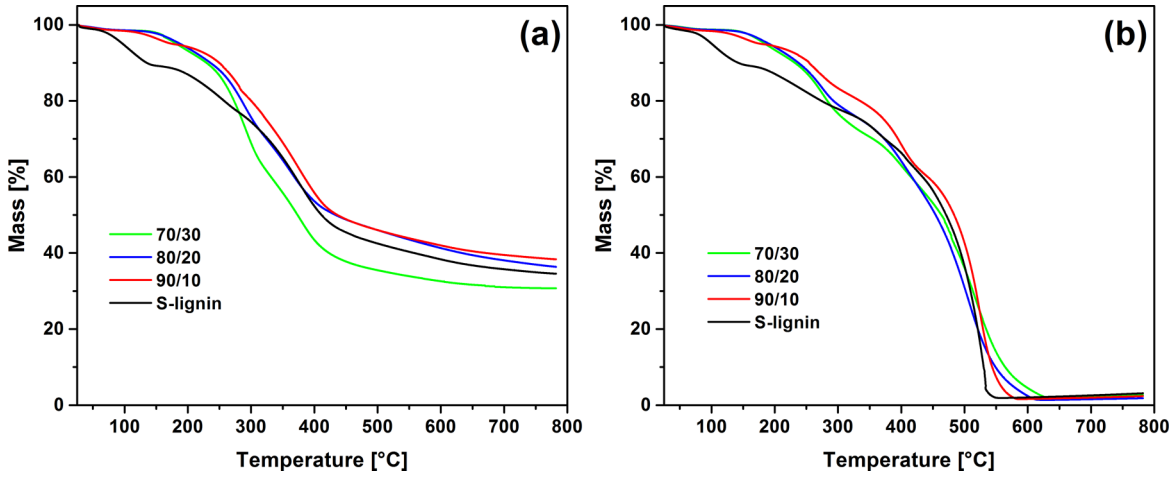

Figure 4. TGA curves under stream of (a) nitrogen and (b) air of MeTHF-soluble lignin fraction (S-lignin) and of lignin-based PU materials at varying S-lignin/TDI weight ratios (70/30, 80/20, 90/10).

methanol has a slightly higher T_g (95 °C). Upon cross-linking, an increase of T_g in the PU materials is found compared with the S-lignin material, which is found to scale with the amount of TDI in the PU; no phase segregation (i.e., other T_g's) are seen. In particular, T_g values of 109, 128 and 143 °C are obtained for 90/10, 80/20 and 70/30 PU systems, respectively. The progressive increase in T_g observed in the PU materials at increasing TDI content may be related to the increasingly stronger intermolecular interactions between the components in the PU materials, such as hydrogen bonding between unreacted OH groups in lignin and urethane cross-linking groups. In the attempt to relate the T_g of the cross-linked S-lignin/TDI system to its composition, the simplified Couchman–Karasz equation:[47]

$$T_g = \frac{w_A T_{gA} + (1 - w_A)(\Delta Cp_B/\Delta Cp_A)T_{gB}}{w_A + (1 - w_A)(\Delta Cp_B/\Delta Cp_A)} \quad (2)$$

was considered, with T_g, T_{gA}, T_{gB}, w_A, ΔCp_A and ΔCp_B ($k_{CK} = \Delta Cp_B/\Delta Cp_A$) being the glass transition temperature of the copolymer, the glass transition temperature of S-lignin, the glass transition temperature of TDI, the mass fraction of S-lignin in the S-lignin/TDI system, the specific heat capacity increment of S-lignin and of TDI at the glass transition (as obtained from DSC measurements), respectively.

As shown in Figure 3b, the experimental data obtained from DSC measurements show a strong positive deviation with respect to the theoretical values predicted by the Couchman–Karasz equation. These results may be explained by considering that the cross-linked S-lignin/TDI system is characterized by strong intermolecular interactions between the two components (viz., strong hydrogen bonds) originating from the presence of urethane groups as cross-links and phenolic/aliphatic hydroxyls in lignin. Such intermolecular interactions may affect the enthalpy of mixing and the excess mixing entropy of the system at the glass-to-liquid transition,[48−51] thus resulting in the observed deviations.

Thermogravimetric Analysis (TGA). TGA measurements were performed to evaluate the thermal stability of these materials, and the results are presented in Figure 4 where TGA traces under both nitrogen (N_2) and air flux are shown. The parent S-lignin material shows three main thermal degradation phenomena during thermolysis under N_2 in the 70–150 °C range, the 150–300 °C range and for temperatures higher than 300 °C (Figure 4a). The first weight loss event accounts for about 15% of mass reduction in S-lignin and may be ascribed to evaporation of trapped solvent and water. The second degradation step yields another 15% mass loss and may be associated with the breaking of α- and β-aryl-alkyl-ether linkages, aliphatic chains and decarboxylation reactions.[31] Finally, the third broad and sharp mass loss event (above 300 °C) may be related to the rupture of carbon–carbon linkages between lignin structural units and functional groups (phenolic hydroxyl groups, carbonyl groups, benzylic hydroxyl groups).[52] Upon cross-linking, improved thermal stability at low temperature (<300 °C) is observed for all PU materials irrespective of the S-lignin/TDI weight ratio, as also indicated by the higher decomposition temperatures at 5% and 10% mass loss found in these systems compared with unreacted S-lignin (see Table 3).

Table 3. Thermal Degradation Temperatures at 5% ($T_{5\%}$), 10% ($T_{10\%}$) and 50% ($T_{50\%}$) Mass Loss, Final Char Residue at 750 °C (R_{750}) and Maximum Mass Loss Derivative Temperature (T_{DTGmax}) for S-lignin and Lignin-based PU Materials at Varying S-lignin/TDI Weight Ratios (70/30, 80/20, 90/10) As Obtained from TGA Measurements under N_2

material	$T_{5\%}$ [°C]	$T_{10\%}$ [°C]	$T_{50\%}$ [°C]	R_{750} [%]	T_{DTGmax} [°C]
70/30	182	230	373	31	290
80/20	188	236	434	37	290
90/10	175	250	437	39	379
S-lignin	97	135	411	35	379

By further increasing the temperature, a broad mass loss event is found in all PUs that can be associated with the degradation of the urethane cross-links and the carbon–carbon structure in lignin. In particular, in the case of 70/30 PU material, a sharper mass loss is observed compared to 80/20 and 90/10 PUs, leading to a slightly lower final char residue at 750 °C (see Table 3). This behavior may be correlated with the presence of residual unreacted NCO groups in the 70/30 PU material even after thermal cross-linking, as evidenced by FTIR spectroscopy (see Figure 2). The thermooxidative behavior of all lignin-based PU materials was also investigated by means of TGA in air. As shown in Figure 4b, improved thermal stability of the cross-

Table 4. Static Contact Angles (θ_{H2O}, θ_{CH2I2}), Total Surface Tension (γ) and Its Dispersive (γ^d) and Polar (γ^p) Components of Lignin-based PU Materials at Varying S-lignin/TDI Weight Ratios (70/30, 80/20, 90/10)

S-lignin/TDI [w/w]	θ_{H2O} [deg]	θ_{CH2I2} [deg]	γ [mN/m]	γ^d [mN/m]	γ^p [mN/m]
70/30	84.4 ± 1.1	41.8 ± 0.9	41.0 ± 0.9	38.7 ± 0.8	2.3 ± 0.3
80/20	82.5 ± 0.6	43.4 ± 1.2	40.9 ± 0.7	37.9 ± 0.5	3.0 ± 0.7
90/10	79.8 ± 1.0	42.4 ± 1.0	42.2 ± 1.1	38.4 ± 0.9	3.8 ± 0.7

linked PU systems compared with unreacted S-lignin is observed in this case, in agreement with the trends observed under N_2 atmosphere (for the sake of clarity, the corresponding differential TGA traces in N_2 and air are reported in the Supporting Information). These results further confirm that the cross-linked PU materials with high lignin content allow for improved thermal stability with respect to the parent un-cross-linked S-lignin sample.

Optical Contact Angle. The wettability properties of the surfaces of all lignin-based PUs were investigated by means of static contact angle measurements against water and diiodomethane (CH_2I_2), and the surface tension γ of each system including its dispersive (γ^d) and polar (γ^p) components was calculated using the Owens, Wendt, Rabel and Kaelble (OWRK) method.[53] The results are shown in Table 4. Because of the partial solubility of S-lignin in water and CH_2I_2, no measurements were performed on unreacted S-lignin. All PU materials present a moderate hydrophobic character with water contact angles θ_{H2O} of 84.4°, 82.5° and 78.8° for 70/30, 80/20 and 90/10 systems, respectively. Interestingly, the hydrophobicity of the PU films is found to decrease slightly at increasing lignin content, being maximum for the 70/30 system. This behavior may be correlated with the presence of hydroxyl groups in lignin (as also evidenced by the FTIR spectra in Figure 2), which increase in number for higher lignin content in the PU material, thus allowing relatively stronger interactions of the PU surface with water and consequently lower contact angle in these systems. This is also partly reflected in the slightly higher value of total surface tension γ in 90/10, compared to 70/30 and 80/20, and in the relatively modest increase in the polar component of surface tension γ^p at increasing lignin content in the PU systems.

Atomic Force Microscopy (AFM). To investigate further the surface characteristics of the PU materials, AFM measurements were performed on S-lignin and PU systems at increasing S-lignin/TDI weight ratio. As shown in the topographical AFM images presented in Figure 5, a progressively coarser morphology is found in the films at increasing lignin content in the PU materials, likely indicating worse film-forming properties for lignin as compared with the TDI. In particular, the progressively more evident formation of visible peaks and valleys at the nanoscale with increasing lignin content in the films leads to a corresponding increase in the root-mean-square surface roughness of the films, as indicated in Table 5.

The surface and interface mechanical properties of S-lignin and lignin-based PU materials were investigated by means of force−distance curve measurements by AFM performed in different areas of films spin-coated onto glass substrates. As presented in Table 5, S-lignin presents an elastic modulus of 3.39 GPa, which is in the same order of magnitude of the values found for the PU materials. In addition, no evident trends are observed by varying the S-lignin/TDI weight ratio, likely indicating that the nanomechanical properties of these systems are not greatly affected by the composition of the material at

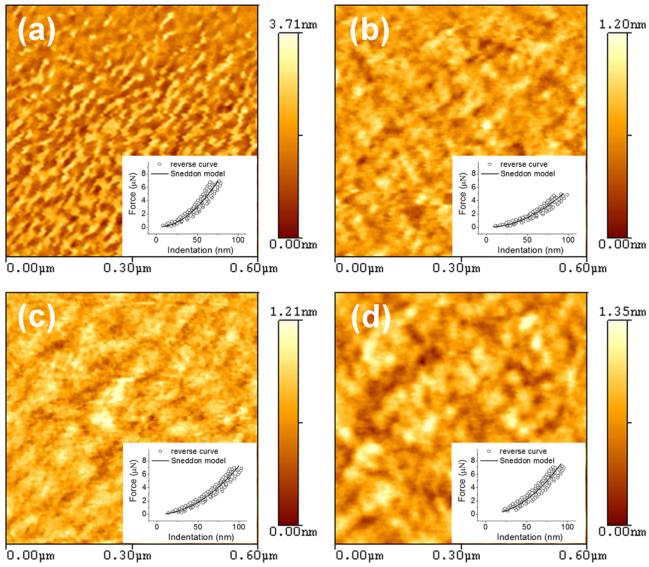

Figure 5. AFM topographical images of lignin-based PU materials at varying S-lignin/TDI ratios ((a) 70/30, (b) 80/20, (c) 90/10) and of (d) S-lignin. The insets to each image show representative indentation-force curves for the systems investigated.

such high lignin contents. The values found on the unreacted lignin sample are in agreement with recent literature reports on analogous systems.[54]

Adhesion Tests. The adhesive strength of cross-linked PU materials was investigated by performing pull-off adhesive tests[38] with the 80/20 cross-linked PU system on different substrates, namely glass, wood, aluminum and steel. As reported in Table 5, the highest adhesive strength is found on wood where cohesive detachment of the substrate during the test was observed, thus indicating very good bonding performance. This result is in agreement with recent literature reports[21] and may be explained by considering the lignocellulosic nature of lignin and its high natural affinity with wood. Similarly, the high adhesion strength observed on glass substrates (7.6 MPa) may be correlated with the high concentration of unreacted hydroxyl groups in the lignin-based PU material, that allow noncovalent interactions with the oxygen groups in glass thus enhancing adhesion on this material. Additionally, the TDI component in the PU system further contributes to its glass adhesion properties. As opposed to this, slightly lower adhesion strengths are observed on metal substrates, with superior performance found on aluminum (1.5 MPa) compared with steel (0.9 MPa). It is however worth noticing that no chemical treatments such as acid pickling were performed on the metal substrates prior to PU deposition and pull-off test. Therefore, further improvements of the adhesive properties of this material on metals may be expected after the application of appropriate metal surface treatments commonly used in industry, due to an increase of metal surface roughness

Table 5. Root-Mean-Square Surface Roughness (As Obtained from Optical Profilometry Measurements), Elastic Modulus (As Obtained from Force-Distance Curve Measurements) of S-lignin and Lignin-based PU Materials at varying S-lignin/TDI Weight Ratios (70/30, 80/20, 90/10) and Adhesive Strength of 80/20 Material on Different Substrates[a]

			pull-off adhesive strength			
S-lignin/TDI [w/w]	surface roughness [μm]	elastic modulus [GPa]	glass [MPa]	wood [MPa]	aluminum [MPa]	steel [MPa]
70/30	0.07 ± 0.01	3.70 ± 0.75				
80/20	0.08 ± 0.02	1.93 ± 0.51	7.6 ± 0.5	>9[b]	1.5 ± 0.3	0.9 ± 0.1
90/10	0.11 ± 0.01	2.10 ± 0.57				
S-lignin	0.20 ± 0.10	3.39 ± 1.18				

[a]The standard deviation is also reported. [b]Cohesive detachment of the substrate (9 MPa represents the maximum allowable instrumental reading).

and available surface area that may lead to a more intimate contact between the PU adhesive and the substrate.

CONCLUSION

New lignin-based thermoset PU coatings with high lignin content were developed and presented in this work. These systems were obtained by extracting the lignin material with a bioderived solvent (MeTHF) and subsequently reacting the MeTHF-soluble fraction with a TDI-based aromatic polyisocyanate at different NCO/OH ratios. Upon solvent extraction, a lower molecular weight lignin fraction with a relatively narrow molecular weight distribution was readily obtained, characterized by a slightly lower concentration of hydroxyl functionalities (8.53 mmol/g) compared with the parent lignin (8.97 mmol/g). FTIR spectroscopy showed that only a minor portion of such OH groups in lignin could directly react with NCO groups to form urethane bonds, likely due to steric hindrance resulting from the highly branched three-dimensional structure of lignin. DSC analysis was used to investigate the thermal transitions in the lignin-based PU materials, and it was shown that higher T_g values could be obtained in the PU materials as compared with the parent MeTHF-soluble lignin. Such improved thermal stability was also confirmed by means of TGA analysis in N_2 and air. Contact angle measurements on the cross-linked lignin-based PU films highlighted a moderately hydrophobic character of these materials. Morphological characterization of the PUs by means of AFM analysis highlighted a progressively coarser morphology in the PU films at increasing lignin content, likely resulting from the relatively poor film-forming properties of high T_g lignin. To evaluate the mechanical properties of the lignin-based PU films, AFM force−distance curves were recorded at different lignin/TDI weight ratios and values of elastic modulus in the range of 2−4 GPa were found on all systems, thus indicating that the nanomechanical properties of these systems are not greatly affected by the composition of the material at such high lignin contents. Finally, the lignin-based PU materials were found to present interesting adhesive properties on different substrate materials, including glass, wood and metals.

The results of this study demonstrate that the direct reaction of chemically unmodified fractionated lignin with polyisocyanates may represent a viable strategy for the development of advanced lignin-based PU thermosetting systems and highlight the potential of lignin-based thermoset PUs as sustainable bioderived materials for application in the field of high-performance coatings and adhesives.

ASSOCIATED CONTENT

Supporting Information

Molecular structure of the TDI-TMP adduct of Desmodur L75, FTIR spectra of S-lignin and of the THF-extracted sol fraction, differential thermal gravimetric analysis curves of lignin-based polyurethane systems performed in nitrogen and air. This material is available free of charge via the Internet at http://pubs.acs.org.

AUTHOR INFORMATION

Corresponding Author

*Gianmarco Griffini. E-mail: gianmarco.griffini@polimi.it. Tel: +39 022399 3213.

Notes

The authors declare no competing financial interest.

ACKNOWLEDGMENTS

This project was funded by the European Commission's Seventh Framework Programme for research, technological development and demonstration under grant agreement no FP7-KBBE-2013-7-613802 ("ValorPlus - Valorisation of biorefinery by-products leading to closed loop systems with improved economic and environmental performance"). The authors gratefully acknowledge Gigliola Clerici for support with GPC and thermal analysis. Prof. Andrea Mele, Prof. Paola D'Arrigo and their collaborators are acknowledged for assistance with ^{13}C NMR measurements.

REFERENCES

(1) Ragauskas, A. J.; Beckham, G. T.; Biddy, M. J.; Chandra, R.; Chen, F.; Davis, M. F.; Davison, B. H.; Dixon, R. A.; Gilna, P.; Keller, M.; Langan, P.; Naskar, A. K.; Saddler, J. N.; Tschaplinski, T. J.; Tuskan, G. A.; Wyman, C. E. Lignin valorization: Improving lignin processing in the biorefinery. *Science* **2014**, *344* (6185), 1246843-1−1246843-10.

(2) Tuck, C. O.; Pérez, E.; Horváth, I. T.; Sheldon, R. A.; Poliakoff, M. Valorization of biomass: Deriving more value from waste. *Science* **2012**, *337* (6095), 695−699.

(3) Lora, J. H.; Glasser, W. G. Recent industrial applications of lignin: A sustainable alternative to nonrenewable materials. *J. Polym. Environ.* **2002**, *10* (1−2), 39−48.

(4) Belgacem, M. N.; Blayo, A.; Gandini, A. Organosolv lignin as a filler in inks, varnishes and paints. *Ind. Crops Prod.* **2003**, *18* (2), 145−153.

(5) Laurichesse, S.; Avérous, L. Chemical modification of lignins: Towards biobased polymers. *Prog. Polym. Sci.* **2014**, *39* (7), 1266−1290.

(6) Thakur, V. K.; Thakur, M. K.; Raghavan, P.; Kessler, M. R. Progress in green polymer composites from lignin for multifunctional applications: A review. *ACS Sustainable Chem. Eng.* **2014**, *2* (5), 1072−1092.

(7) Auvergne, R.; Caillol, S.; David, G.; Boutevin, B.; Pascault, J.-P. Biobased thermosetting epoxy: Present and future. *Chem. Rev.* **2013**, *114* (2), 1082−1115.
(8) El Mansouri, N. E.; Yuan, Q.; Huang, F. Synthesis and characterization of kraft lignin-based epoxy resins. *BioResources* **2011**, *6* (3), 2492−2503.
(9) Ismail, T. N. M. T.; Hassan, H. A.; Hirose, S.; Taguchi, Y.; Hatakeyama, T.; Hatakeyama, H. Synthesis and thermal properties of ester-type crosslinked epoxy resins derived from lignosulfonate and glycerol. *Polym. Int.* **2010**, *59* (2), 181−186.
(10) Sun, G.; Sun, H.; Liu, Y.; Zhao, B.; Zhu, N.; Hu, K. Comparative study on the curing kinetics and mechanism of a lignin-based-epoxy/anhydride resin system. *Polymer* **2007**, *48* (1), 330−337.
(11) Vilela, C.; Sousa, A. F.; Fonseca, A. C.; Serra, A. C.; Coelho, J. F. J.; Freire, C. S. R.; Silvestre, A. J. D. The quest for sustainable polyesters - Insights into the future. *Polym. Chem.* **2014**, *5* (9), 3119−3141.
(12) Luong, N.; Binh, N.; Duong, L.; Kim, D.; Kim, D.-S.; Lee, S.; Kim, B.; Lee, Y.; Nam, J.-D. An eco-friendly and efficient route of lignin extraction from black liquor and a lignin-based copolyester synthesis. *Polym. Bull.* **2012**, *68* (3), 879−890.
(13) Thanh Binh, N. T.; Luong, N. D.; Kim, D. O.; Lee, S. H.; Kim, B. J.; Lee, Y. S.; Nam, J.-D. Synthesis of lignin-based thermoplastic copolyester using kraft lignin as a macromonomer. *Compos. Interfaces* **2009**, *16* (7−9), 923−935.
(14) Kang, Y.; Chen, Z.; Wang, B.; Yang, Y. Synthesis and mechanical properties of thermoplastic films from lignin, sebacic acid and poly(ethylene glycol). *Ind. Crops Prod.* **2014**, *56* (0), 105−112.
(15) Evtugin, D. V.; Gandini, A. Polyesters based on oxygen-organosolv lignin. *Acta Polym.* **1996**, *47* (8), 344−350.
(16) Doherty, W. O. S.; Mousavioun, P.; Fellows, C. M. Value-adding to cellulosic ethanol: Lignin polymers. *Ind. Crops Prod.* **2011**, *33* (2), 259−276.
(17) Hu, L.; Pan, H.; Zhou, Y.; Zhang, M. Methods to improve lignin's reactivity as a phenol substitute and as replacement for other phenolic compounds: A brief review. *BioResources* **2011**, *6* (3), 3515−3525.
(18) Pérez, J. M.; Rodríguez, F.; Alonso, M. V.; Oliet, M. Time−temperature−transformation cure diagrams of phenol−formaldehyde and lignin−phenol−formaldehyde novolac resins. *J. Appl. Polym. Sci.* **2011**, *119* (4), 2275−2282.
(19) Xue, B.-L.; Wen, J.-L.; Zhu, M.-Q.; Sun, R.-C. Lignin-based polyurethane film reinforced with cellulose nanocrystals. *RSC Adv.* **2014**, *4* (68), 36089−36096.
(20) Xue, B.-L.; Wen, J.-L.; Sun, R.-C. Lignin-based rigid polyurethane foam reinforced with pulp fiber: Synthesis and characterization. *ACS Sustainable Chem. Eng.* **2014**, *2* (6), 1474−1480.
(21) Chauhan, M.; Gupta, M.; Singh, B.; Singh, A. K.; Gupta, V. K. Effect of functionalized lignin on the properties of lignin−isocyanate prepolymer blends and composites. *Eur. Polym. J.* **2014**, *52* (0), 32−43.
(22) Jeong, H.; Park, J.; Kim, S.; Lee, J.; Ahn, N.; Roh, H.-g. Preparation and characterization of thermoplastic polyurethanes using partially acetylated kraft lignin. *Fibers Polym.* **2013**, *14* (7), 1082−1093.
(23) Cateto, C. A.; Barreiro, M. F.; Rodrigues, A. E.; Belgacem, M. N. Kinetic study of the formation of lignin-based polyurethanes in bulk. *React. Funct. Polym.* **2011**, *71* (8), 863−869.
(24) Cateto, C. A.; Barreiro, M. F.; Rodrigues, A. E.; Brochier-Salon, M. C.; Thielemans, W.; Belgacem, M. N. Lignins as macromonomers for polyurethane synthesis: A comparative study on hydroxyl group determination. *J. Appl. Polym. Sci.* **2008**, *109* (5), 3008−3017.
(25) Hatakeyama, H. Hatakeyama, T. Lignin Structure, Properties, and Applications. In *Biopolymers*; Abe, A., Dusek, K., Kobayashi, S., Eds.; Springer: Berlin, Germany, 2010, Vol. *232*, pp 1−63.
(26) Cinelli, P.; Anguillesi, I.; Lazzeri, A. Green synthesis of flexible polyurethane foams from liquefied lignin. *Eur. Polym. J.* **2013**, *49* (6), 1174−1184.
(27) Yang, L.; Wang, X.; Cui, Y.; Tian, Y.; Chen, H.; Wang, Z. Modification of renewable resources—lignin—by three chemical methods and its applications to polyurethane foams. *Polym. Adv. Technol.* **2014**, *25* (10), 1089−1098.
(28) Hatakeyama, H.; Hirogaki, A.; Matsumura, H.; Hatakeyama, T. Glass transition temperature of polyurethane foams derived from lignin by controlled reaction rate. *J. Therm. Anal. Calorim.* **2013**, *114* (3), 1075−1082.
(29) Li, Y.; Ragauskas, A. J. Kraft lignin-based rigid polyurethane foam. *J. Wood Chem. Technol.* **2012**, *32* (3), 210−224.
(30) Cateto, C. A.; Barreiro, M. F.; Ottati, C.; Lopretti, M.; Rodrigues, A. E.; Belgacem, M. N. Lignin-based rigid polyurethane foams with improved biodegradation. *J. Cell. Plast.* **2014**, *50* (1), 81−95.
(31) Ciobanu, C.; Ungureanu, M.; Ignat, L.; Ungureanu, D.; Popa, V. I. Properties of lignin−polyurethane films prepared by casting method. *Ind. Crops Prod.* **2004**, *20* (2), 231−241.
(32) Saito, T.; Brown, R. H.; Hunt, M. A.; Pickel, D. L.; Pickel, J. M.; Messman, J. M.; Baker, F. S.; Keller, M.; Naskar, A. K. Turning renewable resources into value-added polymer: Development of lignin-based thermoplastic. *Green Chem.* **2012**, *14* (12), 3295−3303.
(33) Saito, T.; Perkins, J. H.; Jackson, D. C.; Trammel, N. E.; Hunt, M. A.; Naskar, A. K. Development of lignin-based polyurethane thermoplastics. *RSC Adv.* **2013**, *3* (44), 21832−21840.
(34) Thring, R. W.; Vanderlaan, M. N.; Griffin, S. L. Polyurethanes from Alcell® lignin. *Biomass Bioenergy* **1997**, *13* (3), 125−132.
(35) Vanderlaan, M. N.; Thring, R. W. Polyurethanes from Alcell® lignin fractions obtained by sequential solvent extraction. *Biomass Bioenergy* **1998**, *14* (5−6), 525−531.
(36) Tan, T. T. M. Cardanol−lignin-based polyurethanes. *Polym. Int.* **1996**, *41* (1), 13−16.
(37) Gu, Y.; Jerome, F. Bio-based solvents: An emerging generation of fluids for the design of eco-efficient processes in catalysis and organic chemistry. *Chem. Soc. Rev.* **2013**, *42* (24), 9550−9570.
(38) *Standard Test Method for Pull-off Strength of Coatings Using Portable Adhesion Testers*; ASTM D4541-09; ASTM International: West Conshohocken, PA, 2009.
(39) *Standard Practice for Assessing the Solvent Resistance of Organic Coatings Using Solvent Rubs*; ASTM D5402-93; ASTM International: West Conshohocken, PA,1999.
(40) Sader, J. E.; Sanelli, J. A.; Adamson, B. D.; Monty, J. P.; Wei, X.; Crawford, S. A.; Friend, J. R.; Marusic, I.; Mulvaney, P.; Bieske, E. J. Spring constant calibration of atomic force microscope cantilevers of arbitrary shape. *Rev. Sci. Instrum.* **2012**, *83* (10), 103705-1−103705-16.
(41) Sneddon, I. N. The relation between load and penetration in the axisymmetric boussinesq problem for a punch of arbitrary profile. *Int. J. Eng. Sci.* **1965**, *3* (1), 47−57.
(42) Cousins, W. J.; Armstrong, R. W.; Robinson, W. H. Young's modulus of lignin from a continuous indentation test. *J. Mater. Sci.* **1975**, *10* (10), 1655−1658.
(43) Suriano, R.; Credi, C.; Levi, M.; Turri, S. AFM nanoscale indentation in air of polymeric and hybrid materials with highly different stiffness. *Appl. Surf. Sci.* **2014**, *311* (0), 558−566.
(44) Saito, T.; Perkins, J. H.; Vautard, F.; Meyer, H. M.; Messman, J. M.; Tolnai, B.; Naskar, A. K. Methanol fractionation of softwood kraft lignin: Impact on the lignin properties. *ChemSusChem* **2014**, *7* (1), 221−228.
(45) Thielemans, W.; Wool, R. P. Lignin esters for use in unsaturated thermosets: Lignin modification and solubility modeling. *Biomacromolecules* **2005**, *6* (4), 1895−1905.
(46) Duval, A.; Lawoko, M. A review on lignin-based polymeric, micro- and nano-structured materials. *React. Funct. Polym.* **2014**, *85* (0), 78−96.
(47) Couchman, P. R.; Karasz, F. E. A classical thermodynamic discussion of the effect of composition on glass-transition temperatures. *Macromolecules* **1978**, *11* (1), 117−119.
(48) Lu, X.; Weiss, R. A. Relationship between the glass transition temperature and the interaction parameter of miscible binary polymer blends. *Macromolecules* **1992**, *25* (12), 3242−3246.

(49) Lienhard, D. M.; Zobrist, B.; Zuend, A.; Krieger, U. K.; Peter, T. Experimental evidence for excess entropy discontinuities in glass-forming solutions. *J. Chem. Phys.* **2012**, *136* (7), 074515-1−074515-9.
(50) Painter, P. C.; Graf, J. F.; Coleman, M. M. Effect of hydrogen bonding on the enthalpy of mixing and the composition dependence of the glass transition temperature in polymer blends. *Macromolecules* **1991**, *24* (20), 5630−5638.
(51) Pinal, R. Entropy of mixing and the glass transition of amorphous mixtures. *Entropy* **2008**, *10* (3), 207−223.
(52) Domínguez, J. C.; Oliet, M.; Alonso, M. V.; Gilarranz, M. A.; Rodríguez, F. Thermal stability and pyrolysis kinetics of organosolv lignins obtained from *Eucalyptus globulus*. *Ind. Crops Prod.* **2008**, *27* (2), 150−156.
(53) Chan, C.-M. *Polymer Surface Modification and Characterization*; Hanser Gardner Publications: Munich, 1993.
(54) Kläusler, O.; Bergmeier, W.; Karbach, A.; Meckel, W.; Mayer, E.; Clauß, S.; Niemz, P. Influence of N,N-dimethylformamide on one-component moisture-curing polyurethane wood adhesives. *Int. J. Adhes. Adhes.* **2014**, *55* (0), 69−76.